Supplementary material

Chemical recycling of the wasted anodic electrolyte from TiO_2 nanotube preparation process to synthesize facet-controlled TiO_2 single crystals as an efficient photocatalyst

Ai-Yong Zhang, Lu-Lu Long, Chang Liu, Wen-Wei Li, Han-Qing Yu*

Department of Chemistry, University of Science and Technology of China, Hefei, 230026, China

1. Preparation of anodic electrolyte

The anodization process was carried out in a voltage-regulated mode. A home-made two-electrode configuration was adopted, and Ti foils were used for both anode and cathode. Initially, a 0.30-mm Ti foil was burnished and immersed in the chemical polishing solution ($HF:HNO_3:H_2O$ = 1:1:2, in volume ratio) to remove oxide layer and blot, and finally cleaned with soap, acetone and isopropanol before and after chemical polishing. Later, anodization was conducted in 0.09 M NH_4F solution (prepared using 8 ml de-ionized water and 72 ml ethylene glycol as the mixed solvent) under continuous stirring. All electrolytes were prepared from reagent grade chemicals. The electrochemical treatment was conducted by applying a potential scanning from the open-circuit potential first to 80 V for 2 min, then to 70 V for 2 min, 60 V for 2 min and 50 V for 2 min, then repeated this voltage-regulated process and finally to 40 V for 120 min at ambient temperature (20 ± 3 ºC).

The voltage-regulated anodization produced a TNTs stratification layer of approximately 7-8 μm and a milk-like wasted electrolyte (Fig. S1). The stratification layer might be generated when stepping initially to a lower voltage and keeping for a time period to sufficiently establish its diffusion and field conditions, and then stepping back to the original high voltage,[1] and it usually possessed a high photoactivity for various environmental applications.[2,3]

2. Preparation of TiO_2 nanocrystals

2.1. Effect of calcination temperature on TiO_2 nanocrystals

23 Calcinating at relatively low temperature, such as 300, 400 and 450°C, the
24 obtained TiO_2 nanoparticles were covered by the residual carbon from anodic
25 ethylene glycol electrolyte due to the incomplete carbonization (Fig. S4C). Samples
26 prepared under these conditions were poorly dispersed and did not show any one
27 single nanocrystal as well as photoactivity. Organic removals on these photocatalysts
28 were attributed mainly to the physical adsorption by the residual carbon.

29 When the calcination temperature was too high, e.g., 700 and 800°C, the as-
30 prepared TiO_2 nanocrystals were not individually dispersed. Instead, they were easily
31 connected with each other along [001] direction to minimize the surface free energy,
32 resulting in the formation of mesopores.[4-6] Certainly, the particles would shrink and
33 decreased the particle size from micronmeter (TiO_2 polycrystalline) to nanometer
34 scale (TiO_2 nanocrystalline) (Fig. S4D-H). This inevitably resulted in space between
35 nanocrystals to create the porous structure in the TiO_2 nanocrystals.

36

37 *2.2. Effect of temperature ramping rate on TiO_2 nanocrystals*

38 At relatively low temperature ramping rates, e.g., 1, 3 and 5 °C/min, the retention
39 times of the two function reactants (F and ethylene glycol) were sufficiently short to
40 accomplish "dissolution-recrystallization" reaction and enable the formation of TiO_2
41 nanocrystals (Fig. S5A-C). However, when the temperature ramping rate was
42 increased to a higher level, e.g., 10 and 20°C/min, the F and ethylene glycol were
43 evaporated out of muffle furnace too slowly and retained within the system too long
44 to retain "dissolution-recrystallization" reaction due to the chemical etching by

excessive F.[7] Thus, the resultant TiO_2 samples showed no single crystal characteristics (Fig. S5D and E).

2.3. Effect of calcination time on TiO_2 nanocrystals

When the sample was calcinated for 1 h, it was too short to accomplish "dissolution-recrystallization" reaction as well as the successful formation of well-dispersed TiO_2 single crystal (Fig. S6A). However, a very long calcination duration would lead to the crystallographic fusion of TiO_2 nanocrystals, increased particle size and pore size, and decreased specific surface area, although the morphology and crystalline phase of TiO_2 remained unchanged (Fig. S6D). Only calcination for 3 and 5 h could cause shrink of TiO_2 particles and lead to a decrease in the particle size from micrometer (TiO_2 polycrystalline) to nanometer scale (TiO_2 nanocrystalline) (Fig. S6B and C).

3. XPS of TiO_2 nanocrystals

The XPS result (Fig. S12A) indicate that the TiO_2 nanocrystal was composed of Ti, O, N, and F elements, and the corresponding photoelectron peaks appeared respectively at binding energies of 458.8 (Ti2p), 529.7 (O1s), 399.5 eV (N1s) and 684.4 (F1s). Ti, O, and F elements should have come from surface fluorinated TiO_2 nanocrystals. N was originated from the self-incorporation into the TiO_2 nanocrystal particles. The atomic ratio of Ti:O was approximately 1:2 (Fig. S12B and C).

The XPS spectrum of N1s core electrons in C-$TiO_{2-x}N_x$ samples exhibited several

binding energies of 399.7, 400.7 and 407.1 eV (Fig. S12D), respectively. Specifically, the N1s peak at 399.7 and 400.7 eV were attributed to the incorporated nitrogen in titania as interstitial N or O-Ti-N, while the N1s peak at 407.1 eV should be originated from surface-adsorbed or contaminated nitrogen species.[8,9]

The XPS spectrums of F1s core electrons in $TiO_{2-x}N_x$ and C-$TiO_{2-x}N_x$ samples both showed a binding energy at 684.6 eV (Fig. S12E), which is a typical value for fluorated TiO_2 systems and could be ascribed to F^- ions physically adsorbed on the TiO_2 surface (such as the surface Ti-F species formed by ligand exchange between F^- and surface hydroxyl groups, $\equiv$Ti-OH + F^- $\rightarrow$ $\equiv$Ti-F + OH^-).[10] No signal for F^- in the lattice of TiO_2 (BE = 688.5 eV) was found. Thus, the atomic incorporation of F atoms or their substitution for O atoms in the anatase TiO_2 crystal lattice (doping) can be ruled out. Previous works have demonstrated that the formation of Ti-F bond can significantly lower the surface free energy of the {001} facets and reversely make them more stable than {101} facets, thus enabling the formation of anatase TiO_2 single crystals with a large percentage of reactive {001} facets.[8]

The XPS spectra of C 1s in C-$TiO_{2-x}N_x$ samples showed several peaks at 284.65, 286.05 and ca. 288.5 eV (Fig. S12F), respectively. The C 1s peak at 284.65 eV is usually assigned to adventitious elemental carbon because of the residual carbon from the precursor solution and the hydrocarbon present in the XPS instrument itself, while the peaks at 286.05 and ca. 288.5 eV suggest the existence of carbonate species.[11,12] However, the peak around 281 eV, intrinsically resulting from the Ti-C bond, was not observed in the samples. Thus, all the C was adsorbed onto surface but not doped into

the TiO_2 nanocrystals in our study.

Notes and references

1 P. Roy, S. Berger and P. Schmuki, *Angew. Chem. Int. Ed.*, 2011, **50**, 2904-2939.

2 S. P. Albu, D. Kim and P. Schmuki, *Angew. Chem. Int. Ed.*, 2008, **47**, 1916-1919.

3 D. Kim, A. Ghicov, S. P. Albu and P. Schmuki, *J. Am. Chem. Soc.*, 2008, **130**, 16454-16455.

4 Z. F. Bian, T. Tachikawa and T. Majima, *J. Phys. Chem. Lett.*, 2012, **3**, 1422-1427.

5 K. L. Lv, Q. J. Xiang and J. G. Yu, *Appl. Catal. B.*, 2011, **104**, 275-281.

6 J. Zhu, S. H. Wang, Z. F. Bian, S. H. Xie, C. L. Cai, J. G. Wang, H. G. Yang and H. X. Li, *CrystEngComm*, 2010, **12**, 2219-2224.

7 X. H. Yang, H. G. Yang and C. Z. Li, *Chem. Eur. J.*, 2011, **17**, 6615-6619.

8 G. Liu, H. G. Yang, X. W. Wang, L. N. Cheng, J. Pan, G. Q. Lu and H. M. Cheng, *J. Am. Chem. Soc.*, 2009, **131**, 12868-12869.

9 S. K. Joung, T. Amemiya, M. Murabayashi and K. Itoh, *Chem. Eur. J.*, 2006, **12**, 5526-5534.

10 C. Z. Wen, H. B. Jiang, S. Z. Qiao, H. G. Yang and G. Q. Lu, *J. Mater. Chem.*, 2011, **21**, 7052-7061.

11 X. X. Yang, C. D. Cao, K. Hohn, L. Erickson, R. Maghirang, D. Hamal and K. Klabunde, *J. Catal.*, 2007, **252**, 296-302.

12 D. E. Gu, Y. Lu, B. C. Yang and Y. D. Hu, *Chem. Commun.*, 2008, **21**, 2453-

112 2455.

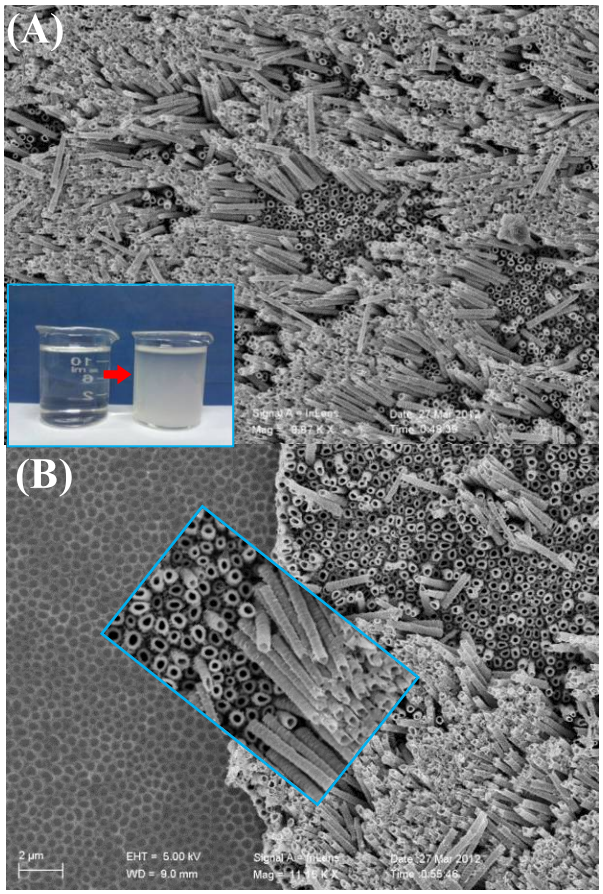

Fig. S1 SEM images of the hierarchical TNTs arrays and optical photon of the residual milk-like electrolyte (inset) from anodization process.

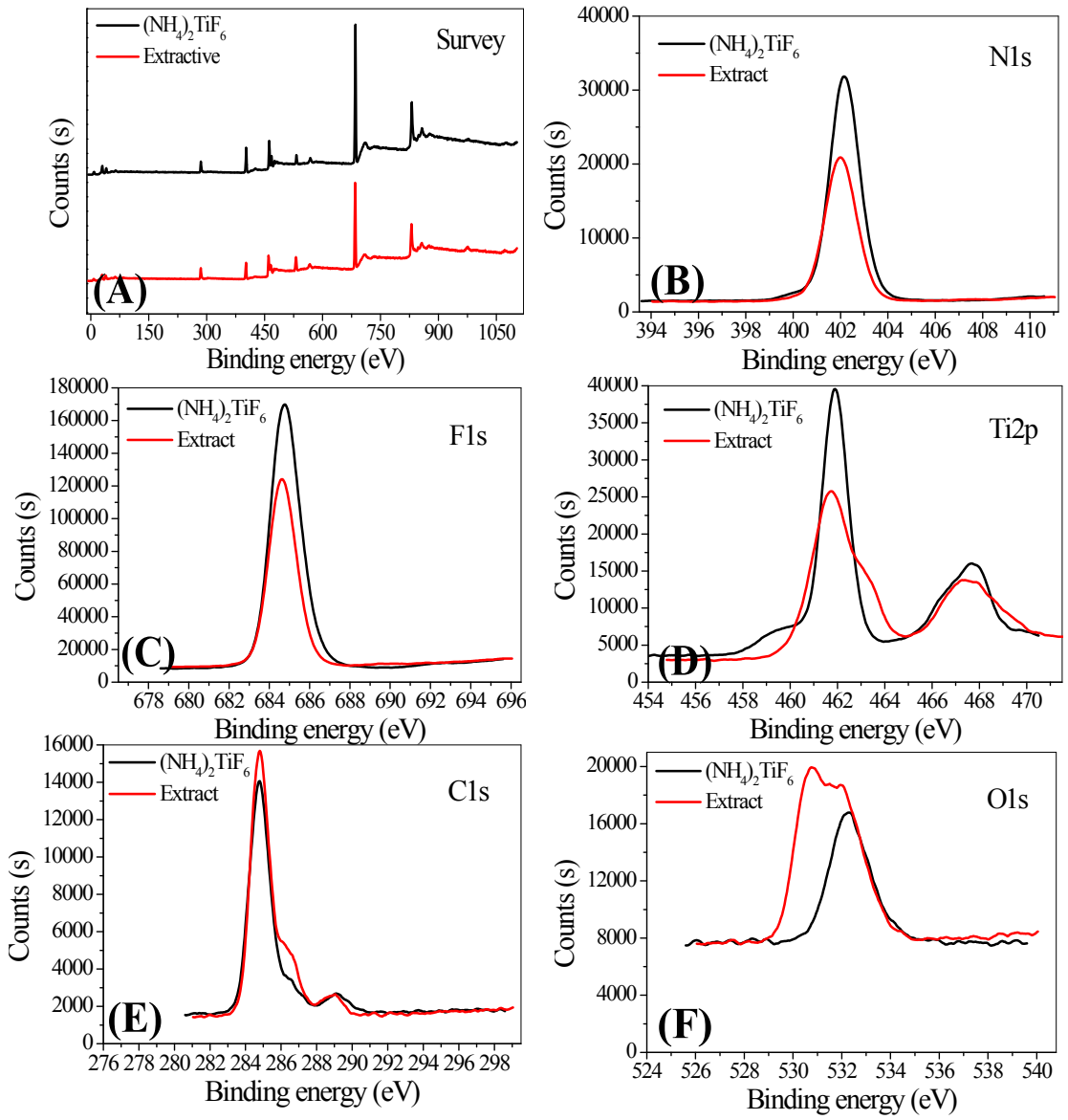

Fig. S2. XPS survey (A) and high-resolution spectras (B, C, D, E and F) for the $(NH_4)_2TiF_6$ and the extract from wasted anodic electrolyte used in this study.

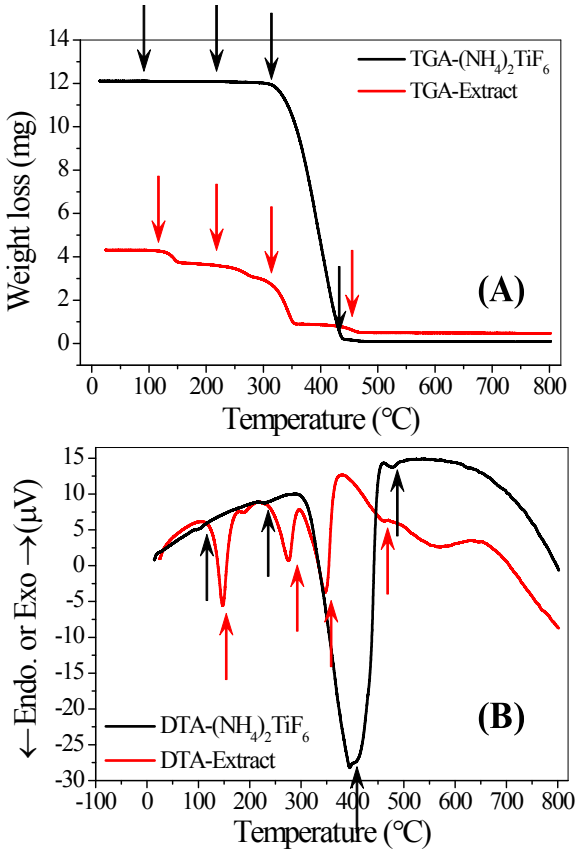

Fig. S3. TGA curves (A) and DTA curves (B) for the $(NH_4)_2TiF_6$ and the extract from wasted anodic electrolyte used in this study.

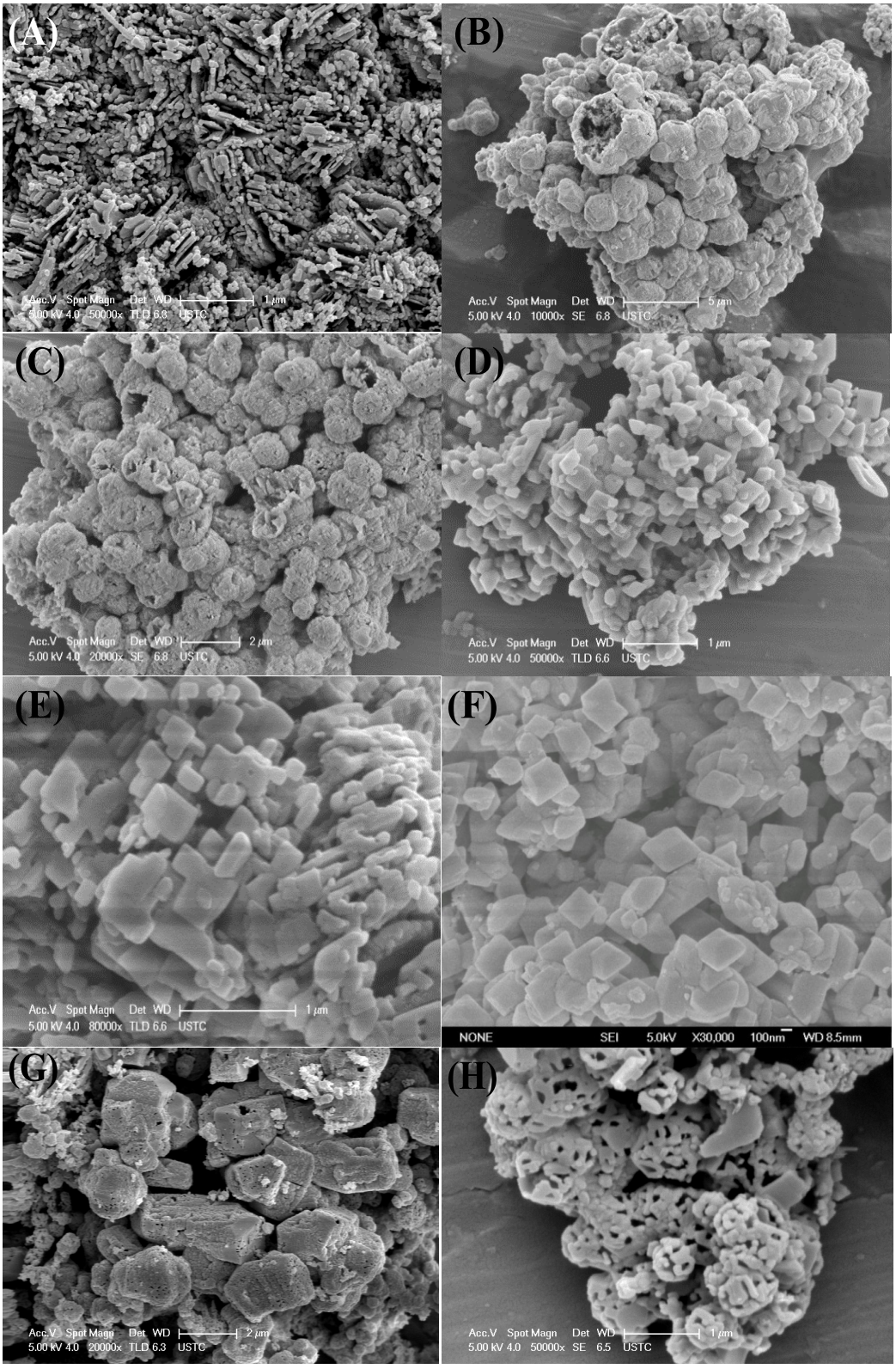

Fig. S4. Typical SEM images of the $TiO_{2-x}N_x$ particles calcinated at different temperatures for 3 h with 5 °C /min: (A) 300°C; (B) 400°C; (C) 450°C; (D) 500°C; (E)

550°C; (F) 600°C; (G) 700°C; and (H) 800°C.

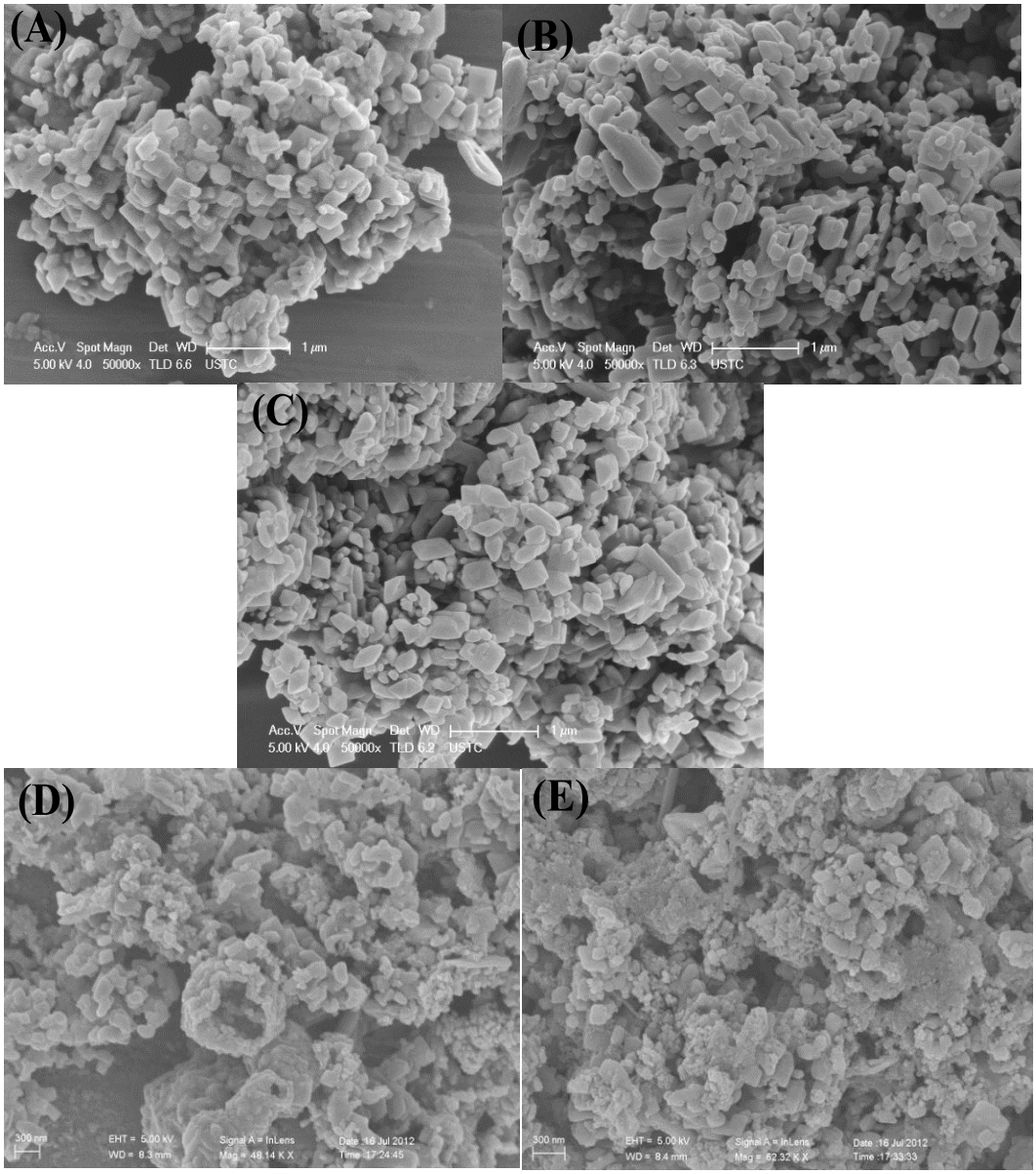

Fig. S5. Typical SEM images of the $TiO_{2-x}N_x$ particles calcinated at 500°C for 3 h with different ramping rates: (A) 1 °C/min; (B) 3 °C/min; (C) 5 °C/min; (D) 10 °C/min; and (E) 20 °C/min.

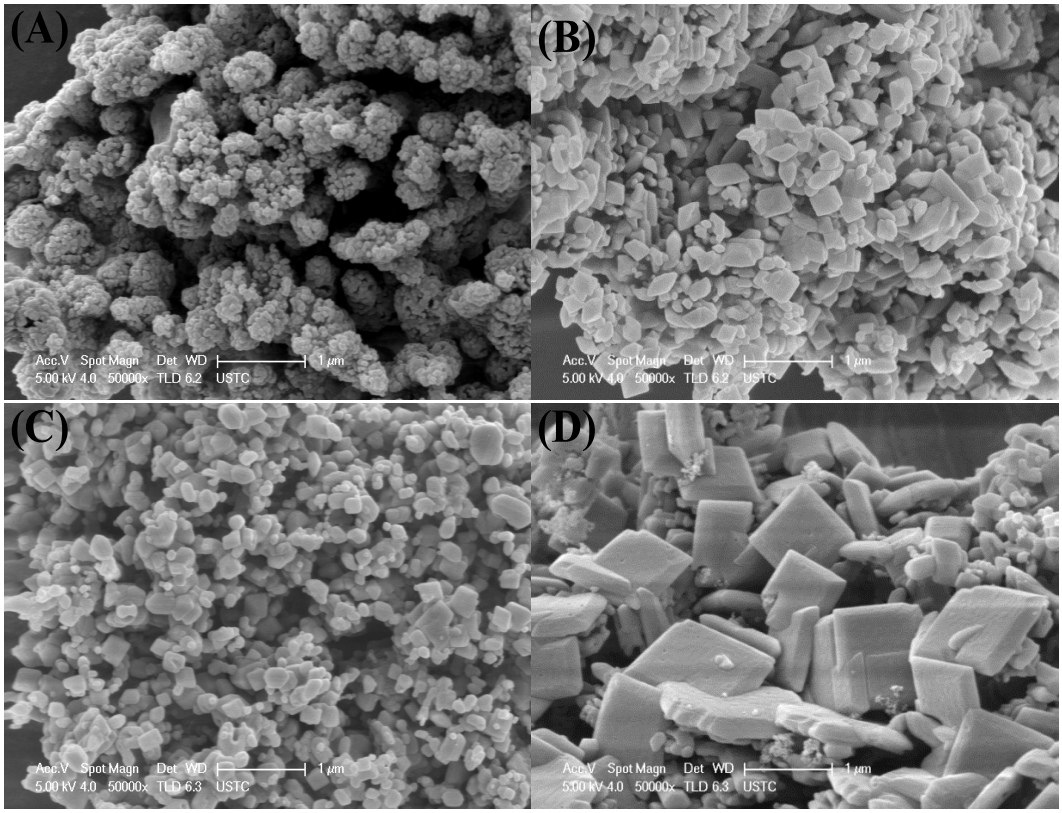

Fig. S6. Typical SEM images of the $TiO_{2-x}N_x$ particles calcinated at 500°C with 5 °C/min for different times: (A) 1 h; (B) 3 h; (C) 5 h; and (D) 8 h.

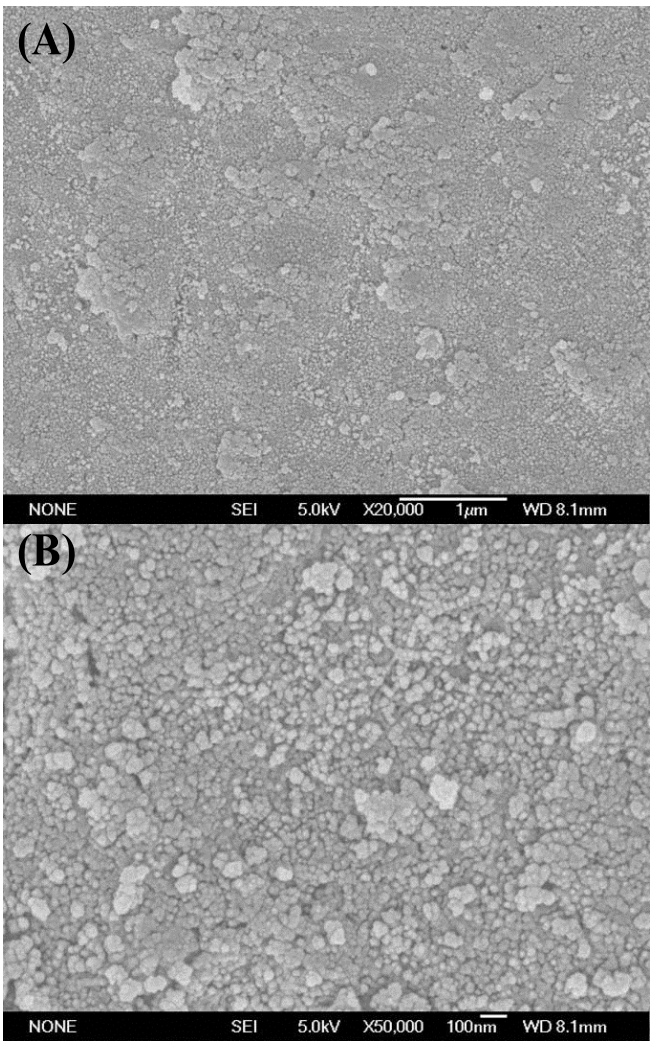

Fig. S7. Typical SEM images of the TiO_2 particles calcinated at 600°C with 5 °C/min from a lowly-concentrated transparent wasted anodic electrolyte (inset): (A) low magnification and (B) high magnification.

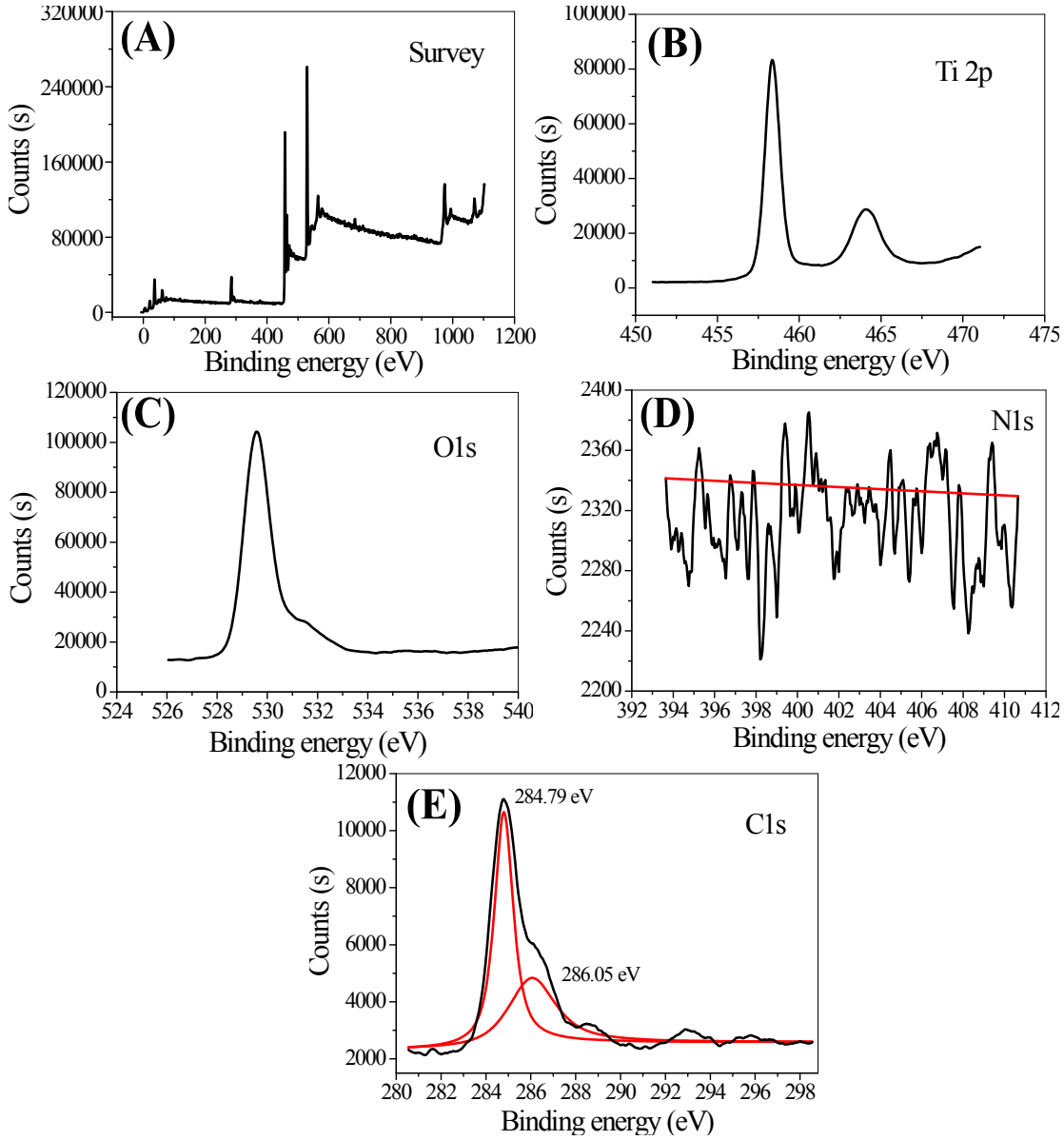

Fig. S8. XPS survey (A) and high-resolution spectras (B, C, D and E) for the TiO_2 nanocrystals prepared by calcinating electrolyte in air at 600 ºC.

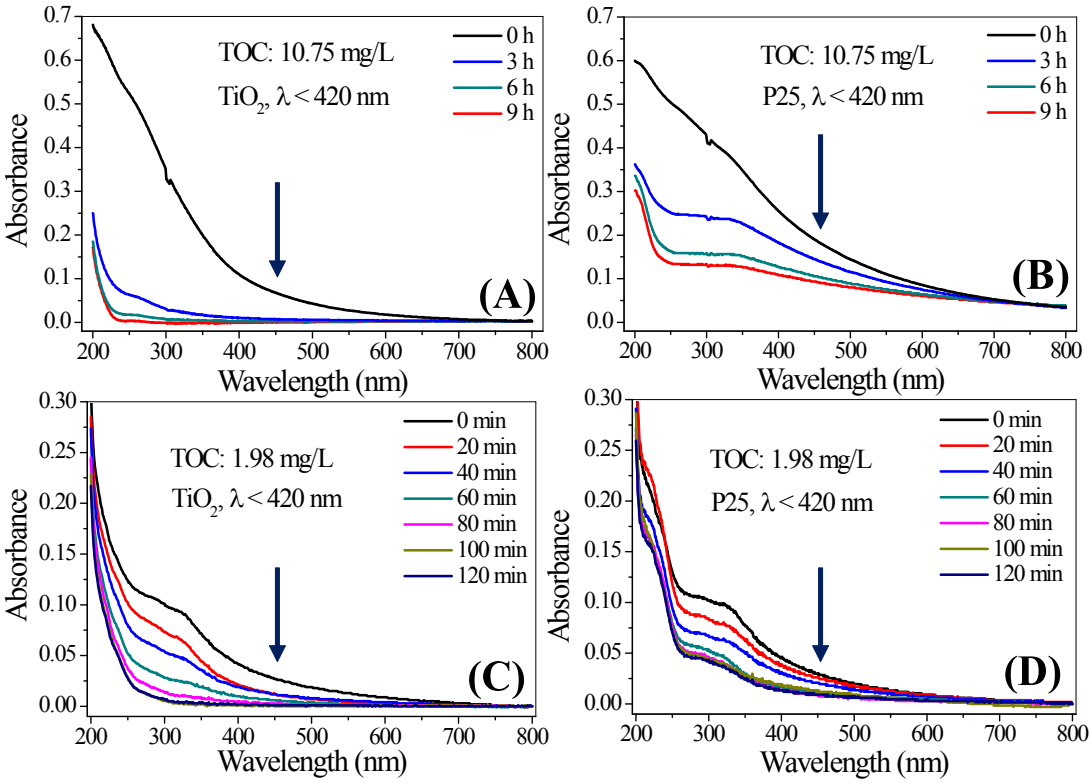

Fig. S9. HAs removal evolutions on the TiO_2 nanocrystals (A and C) and P25 (B and D) under UV irradiation (λ < 420 nm), with an initial TOC concentration of 10.75 and 1.98 mg/L.

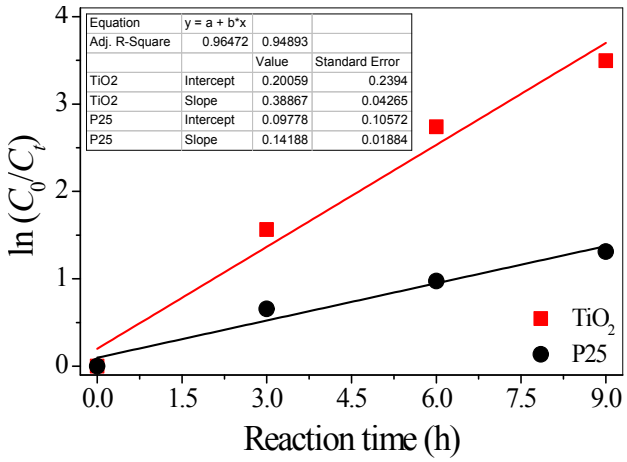

Fig. S10. L-H pseudo-first order HAs degradation kinetics on the TiO_2 nanocrystals and P25 under UV irradiation (λ < 420 nm), with an initial TOC concentration of 10.75 mg/L.

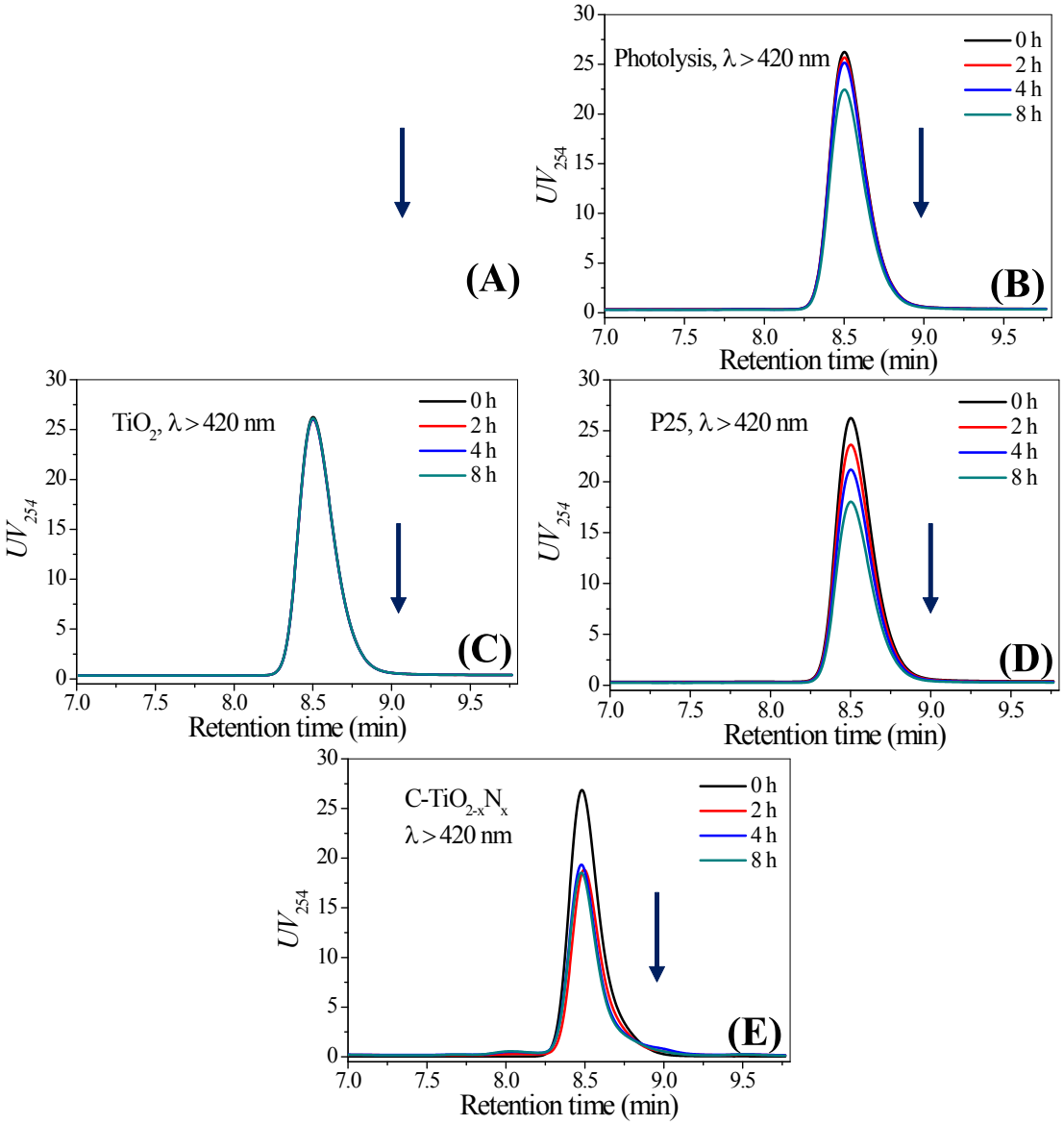

Fig. S11. Bentazone removal evolutions on $TiO_{2-x}N_x$ crystals (A), photolysis (B), TiO_2 crystals (C), P25 (D) and C-$TiO_{2-x}N_x$ crystals (E) under Vis irradiation (λ > 420 nm), with an initial bentazone concentration of 3.0 mg/L.

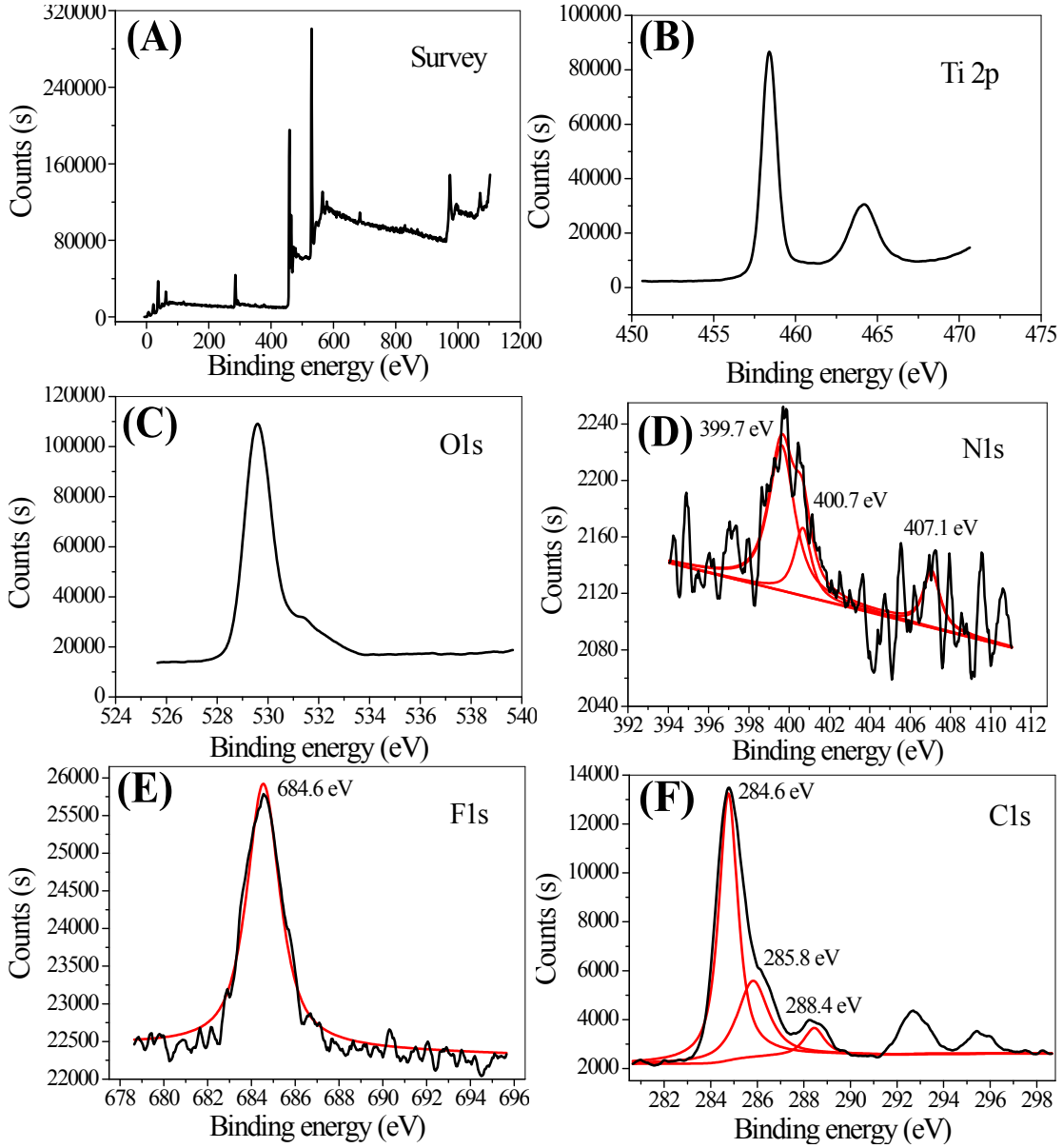

Fig. S12. XPS survey (A) and high-resolution spectras (B, C, D, E and F) for the C-$TiO_{2-x}N_x$ nanocrystals prepared by calcinating electrolyte in air at 400 ºC.

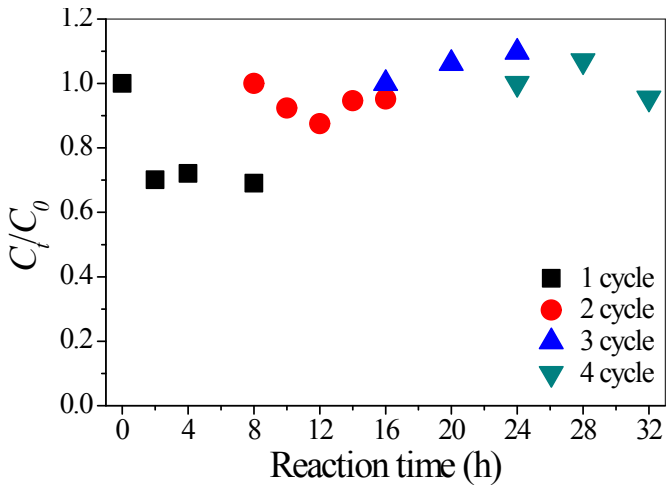

Fig. S13. Cyclic bentazone removal evolutions on C-$TiO_{2-x}N_x$ nanocrystals under Vis irradiation ($\lambda > 420$ nm), with an initial bentazone concentration of 3.0 mg/L.